15th Triennial World Congress, Barcelona, Spain

ON MANIPULATOR CONTROL VIA VELOCITY FIELDS [1]

Javier Moreno and Rafael Kelly

División de Fisica Aplicada, CICESE, Apdo. Postal 2615 Adm. 1
Ensenada, B.C., 22800
MEXICO
fax: +52 (646) 175–05–54
e–mail: rkelly@cicese.mx

Abstract: This paper addresses the control of robotic manipulators using the velocity field approach. Instead of the usual specification in motion robot control via desired position trajectories depending on time, the specification in the velocity field control formulation is given through a desired velocity vector field as a function of actual position regardless of time. This approach is useful for control following task. This paper presents two controllers to solve the velocity field control formulation in task space. Experiments using these controllers on a two degrees–of–freedom direct–drive arm illustrate the feasibility of the proposed approach. *Copyright © 2002 IFAC*

Keywords: Robot control, Stability, Vector field, Velocity field.

1. INTRODUCTION

In the absence of friction and other disturbances, the dynamics of a serial *n*-link robot can be written as (Spong and Vidyasagar, 1989):

$$M(q)\ddot{q} + C(q,\dot{q})\dot{q} + g(q) = \tau \tag{1}$$

where q is the $n \times 1$ vector of joint displacements, $\dot{q}$ is the $n \times 1$ vector of joint velocities, τ is the $n \times 1$ vector of torque inputs, $M(q)$ is the $n \times n$ symmetric positive definite manipulator inertia matrix, $C(q,\dot{q})\dot{q}$ is the $n \times 1$ vector of centripetal and Coriolis torques, and $g(q)$ is the $n \times 1$ vector of gravitational torques due to gravity.

A natural appealing to describe most robot manipulators activities is in task space where position and orientation of the robot end–effector are of concern. Denoting by $h(q) : \mathbb{R}^n \to \mathbb{R}^m$ the robot direct kinematics, then the position and orientation $x \in \mathbb{R}^m$ of the end–effector is given by

$$x = h(q). \tag{2}$$

The time derivative of the direct kinematic model (2) yields the differential kinematic model

$$\dot{x} = \frac{d}{dt}h(q) = \frac{\partial h}{\partial q}\dot{q} = J(q)\dot{q} \tag{3}$$

where $J(q)$ is the so–called analytical Jacobian matrix (Canudas *et al.*, 1996).

The second order kinematics can be obtained by further differentiation, i.e.,

$$\ddot{x} = J(q)\ddot{q} + \dot{J}(q)\dot{q}. \tag{4}$$

Assuming that the analytical Jacobian $J(q)$ is full–rank, thus $J(q)J(q)^T$ is nonsingular (Canudas *et al.*, 1996), and the Jacobian pseudoinverse solution corresponding to (4) is

[1] Work partially supported by CONACyT grant 32613–A and SNI, Mexico.

$$\ddot{q} = J(q)^{\dagger}\left[\ddot{x} - \dot{J}(q)\dot{q}\right], \tag{5}$$

where the pseudoinverse is given be

$$J(q)^{\dagger} = J(q)^{T}\left[J(q)J(q)^{T}\right]^{-1}.$$

The specification of tasks to be executed by manipulators is usually given in terms of desired position trajectories in task space $x_d(t)$. The motion control aim (trajectory tracking) is to achieve asymptotic tracking of the desired position trajectory, that is

$$\lim_{t\to\infty}\left[x_d(t) - x(t)\right] = 0.$$

Contour control of a robot arm is an act of the end–effector tip being moved along a path with an assigned velocity (Nakamura *et al.*, 2000). Contour control is one important goal for machining operations since contouring accuracy is crucial for a precise motion system. Several approaches to improve the contouring accuracy are surveyed in (Chiu, 1998; Li, 1999). Figure 1 depicts the contouring error, which measures the shortest distance between the current end–effector position x and some point in the contour, and the tracking error, which is the deviation between the current position x and the desired location specified by the timed trajectory x_d at the current time.

Velocity field control has been recently introduced by Li and Horowitz (1999), which attempts to be an alternative to motion control. In this control philosophy, the task to be accomplished by the robot is coded by means of a smooth desired *velocity vector field* defined in the task configuration space $\mathscr{G}$ and denoted as a map

$$\begin{array}{rccc} v(x): & \mathscr{G} & \to & T\mathscr{G} \\ & x & \mapsto & v(x) \end{array}$$

where $T_x\mathscr{G}$ is the tangent space of $\mathscr{G}$ at the specific configuration x and $T\mathscr{G} = \cup_{x\in\mathscr{G}} T_x\mathscr{G}$ denotes the tangent bundle of $\mathscr{G}$.

A velocity field defines a tangent vector (the desired end–effector velocity $\dot{x}_d$) at every point of the robot task configuration space. Figure 2 illustrates the specification of motion by means of a velocity field. This Figure depicts a velocity field defined in the task space of a two degrees of freedom robot arm which assigns a desired velocity vector (arrow) to each point in the task space. The flow lines shown in Figure 2 indicate that they converge to a given circular contour.

Although the idea of motion specification independent of time for a robotic task seems at first sight illogical, in many application the timing of the desired trajectory is unimportant compared to the coordination and synchronization requirements between the various degrees of freedom. In this way, velocity field control approach is particularly well suited to contour following tasks for machining operations such as cutting, milling and deburring (Li, 1999).

The velocity field control objective revolves around the computation of the joint torques τ required to

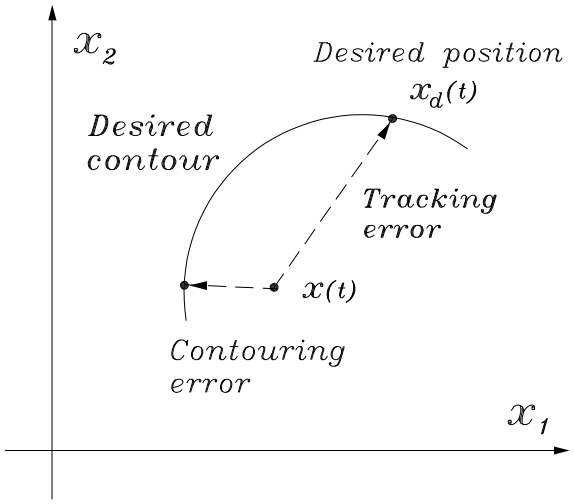

Fig. 1. Tracking and contouring errors

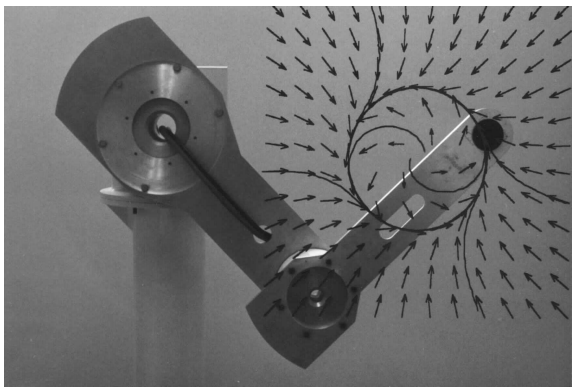

Fig. 2. Desired velocity field in Cartesian space

vanish the velocity field error defined as the difference between the desired velocity field $v(x)$ and the manipulator end–effector velocity $\dot{x}$, that is

$$\lim_{t\to\infty}\left[v(x(t)) - \dot{x}(t)\right] = 0. \tag{6}$$

In this situation the desired velocity field $v(x)$ is defined so that if the velocity $\dot{x}$ of the output matches the velocity field $v(x)$, that is $\dot{x} = v(x)$, then the robot output is guided towards the desired contour. In this sense we say that the desired velocity field encodes the robot task. Thus, instead of requiring the arm end–efector tip to be at specific location at each instant time as it is imposed in trajectory tracking control, in velocity field control the arm tip will match with the flow lines of the desired velocity field, as it can be seen in Figure 2.

The contribution of this paper is twofold. First, we present two control laws to solve the velocity field control formulation without regard of closed–loop passivity requirements. The first controller is based on inverse dynamics whereas the second uses a two–loops control structure involving a joint velocity inner loop better adapted to the kinematic control concept. Second, we have conducted experimental studies on a two degrees–of–freedom direct–drive arm. There, contour control is illustrated through requesting the

task of tracing a circle with constant tangent speed in task space.

2. VELOCITY FIELD CONTROL

2.1 *Inverse dynamics controller*

In order to achieve velocity field control in task space (6) we exploit the inverse dynamic control structure given by

$$\tau = M(q)u_0 + C(q,\dot{q})\dot{q} + g(q) \tag{7}$$

which transforms the robot dynamics (1) into the linear system

$$\ddot{q} = u_0. \tag{8}$$

A new control input u_0 can be chosen by the second-order differential kinematics equation (4). According to the pseudoinverse solution (5), the input

$$u_0 = J(q)^\dagger \left[\frac{\partial v(x)}{\partial x}\dot{x} + K_v[v(x) - \dot{x}] + K_p\xi - \dot{J}(q)\dot{q} \right] \tag{9}$$

$$\xi(t) = \int_0^t [v(x(\sigma)) - \dot{x}(\sigma)]\, d\sigma \tag{10}$$

with K_p and K_v symmetric positive definite matrices, leads to the following closed–loop equation

$$\ddot{\xi} + K_v\dot{\xi} + K_p\xi = 0.$$

This is a lineal system which is globally asymptotically stable. Hence we get the conclusion $\lim_{t\to\infty}\xi(t) = \lim_{t\to\infty}\dot{\xi}(t) = 0$ which implies from (10):

$$\lim_{t\to\infty}[v(x(t)) - \dot{x}(t)] = 0$$

as desired.

2.2 *Two–loops based controller*

One more solution to velocity field control in task space can be extracted from ideas reported in (Kelly *et al.*, 1999) which are closely related to the concept of kinematic control.

Under the optics of kinematic control, the joint velocity $\dot{q}$ can be seen as the robot input. Considering this situation and assuming that the analytical robot Jacobian $J(q)$ is full–rank and bounded, we propose the following control law to generate the desired joint velocity $\dot{q}_d$

$$\dot{q}_d = J(q)^\dagger [v(x) + K\xi] \tag{11}$$

where ξ is given by equation (10) and K is a symmetric positive definite matrix. Under the assumption of exact velocity tracking, i.e., $\dot{q}(t) \equiv \dot{q}_d(t)$, and substituting (11) into (3) we get

$$\frac{d}{dt}\xi = -K\xi$$

and therefore $\lim_{t\to\infty}\xi(t) = 0$ and $\lim_{t\to\infty}\dot{\xi}(t) = 0$ as desired.

However, in practice most joint velocity controllers assure —in the best case— only asymptotic velocity tracking instead of exact tracking. One simple example of asymptotic joint velocity controller can be easily derived from the inverse dynamics approach

$$\tau = M(q)\left[\ddot{q}_d + K_v\tilde{\dot{q}} + K_p z\right] + C(q,\dot{q})\dot{q} + g(q) \tag{12}$$

$$\dot{z} = \tilde{\dot{q}} \tag{13}$$

with K_p and K_v symmetric positive definite matrices. This control scheme requires the desired joint acceleration $\ddot{q}_d(t)$ which is obtained through (11) as

$$\ddot{q}_d = J(q)^\dagger \left[\frac{\partial v(x)}{\partial x}\dot{x} + K[v(x) - \dot{x}] \right] + \left[\frac{d}{dt}J(q)^\dagger \right] [v(x) + K\xi]. \tag{14}$$

In this way a two–loops control scheme is obtained which is expected to drive the velocity field error to zero. To prove this claim, notice that after some manipulations the overall closed–loop system is given by

$$\frac{d}{dt}\begin{bmatrix} z \\ \tilde{\dot{q}} \\ \xi \end{bmatrix} = \begin{bmatrix} 0 & I & 0 \\ -K_p & -K_v & 0 \\ 0 & 0 & -K \end{bmatrix}\begin{bmatrix} z \\ \tilde{\dot{q}} \\ \xi \end{bmatrix} + \begin{bmatrix} 0 \\ 0 \\ J(q)\tilde{\dot{q}} \end{bmatrix}. \tag{15}$$

Observe that the state variables z and $\tilde{\dot{q}}$ are independent of ξ. Indeed, the z and $\tilde{\dot{q}}$ dynamics is characterized by a lineal asymptotically stable system; therefore $\lim_{t\to\infty}\tilde{\dot{q}}(t) = 0$. In this way, $\tilde{\dot{q}}$ vanishes exponentially, the same as the term $J(q)\tilde{\dot{q}}$ because the boundedness assumption on the Jacobian. Hence the total system is globally convergent which allows the conclusion

$$\lim_{t\to\infty}\dot{\xi}(t) = \lim_{t\to\infty}[v(x(t)) - \dot{x}(t)] = 0.$$

3. EXPERIMENTAL RESULTS

The experiments presented in this section have been accomplished on a mechanical arm built at CICESE Research Center. This is a direct–drive vertical arm with two degrees–of–freedom whose rigid links are

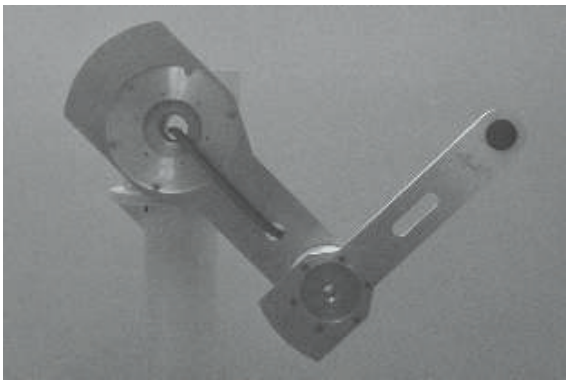

Fig. 3. Experimental robot arm

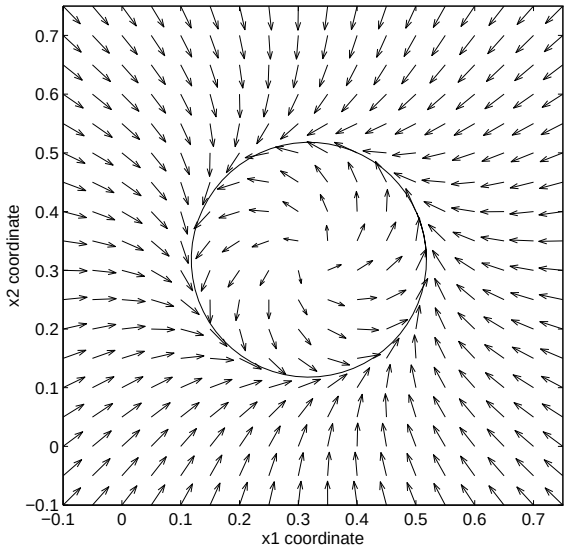

Fig. 4. Vector field used in experiments

joined with revolute joints (see Figure 3). For a complete description and model of the set–up, the reader is refered to (Reyes and Kelly, 1997; Reyes and Kelly, 2001).

Experiments showed that static, Coulomb, and viscous friction at the motor joints are present and they depend in a complex manner on the joint position and velocity. Instead of modeling static and Coulomb friction for compensation purposes, we have decided to consider them as unmodeled dynamics and only viscous friction was compensated.

The control algorithms were written in C programming language executed in the control board at a 2.5 msec. sampling rate.

3.1 *Desired velocity field*

The specified velocity field $v(x)$ should be chosen to exhibit a behavior without abrupt changes in velocity and acceleration such that saturation on actuators is prevented. The proposed velocity field $v(x)$ "draws" a circle in the x_1–x_2 plane as shown in Figure 4 where the corresponding desired speed at each point is approximately 0.1 [m/sec]. The circle center coordinates are x_{c1}=0.318 [m] and x_{c2}=0.318 [m]. The control aim is to drive the arm in such a way that the position of the arm tip follows the velocity field, hence to track asymptotically a circle.

We have conducted two experiments corresponding to the inverse dynamics based controller (7), (9) and (10), and two loops based controller (10)–(13), respectively.

Since tracking position error has nonsense in velocity field control, we have recurred to the contouring error to assess the performance of the velocity field controllers. The contouring error is defined as (Chiu and Tomizuka, 2001)

$$e_C(t) = r_0 - \sqrt{[x_{c1} - x_1(t)]^2 + [x_{c2} - x_2(t)]^2}.$$

The arm initial configuration was at position $x(0)^T = [0.636\ 0]^T$ [m].

3.2 *Inverse dynamics controller*

The first experiment was carried out with the inverse dynamics controller described by equations (7), (9) and (10). The following gains K_p and K_v were used

$$K_p = \text{diag}\{2000, 2000\}\ [\text{Nm/rad}],$$
$$K_v = \text{diag}\{20, 20\}\ [\text{Nm seg/rad}].$$

The contouring error e_C is shown in Figure 5. There are observed peaks in steady state of 0.004 [m], that is a 2 % with respect to the circle radius. Figure 6 shows the path of the robot tip in the x_1–x_2 plane while Figure 7 depicts the evolution of the tip speed $\|\dot{x}\|$. Good performance is observed from Figure 6, however a little deformation is observed in the circle traced by the robot which is due to Coulomb friction present at the arm joints. Figure 7 shows that $\|\dot{x}\|$ has high frequency components which may be due to the simple method based on the Euler approximation to estimate joint velocity $\dot{q}$. By increasing the gains K_p and K_v, experiments demonstrate behavior improvement but high frequency components still appear on $\|\dot{x}\|$ and applied torques τ. Observe that smooth motion transient was presented, and the accomplishment of velocity field control objective allowed to attain the task of tracing a circle with constant speed in a natural fashion.

3.3 *Two–loops based controller*

The second experiment was conducted with the two–loops controller given by (10)–(13) with the following gains

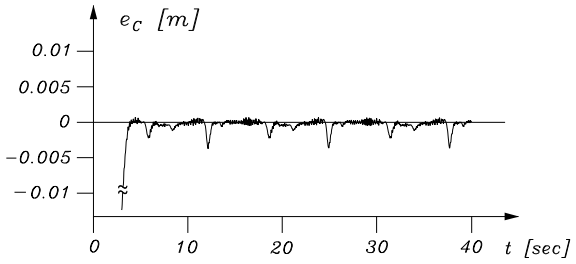

Fig. 5. Contouring error using inverse dynamics based controller

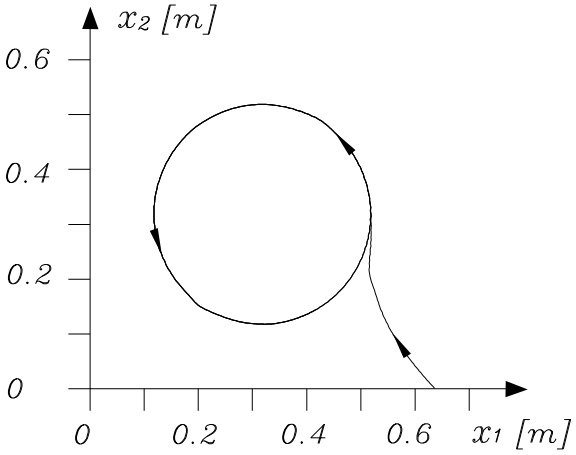

Fig. 6. Path of the arm tip using inverse dynamics based controller

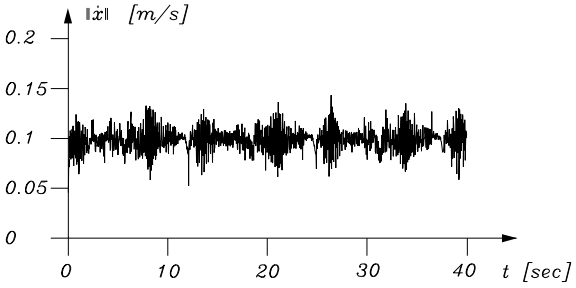

Fig. 7. Speed $\|\dot{x}\|$ using inverse dynamics based controller

$$K_p = \text{diag}\{250, 250\}\ [\text{Nm/rad}],$$
$$K_v = \text{diag}\{30, 30\}\ [\text{Nm seg/rad}],$$
$$K = \text{diag}\{25, 25\}\ [1/\text{sec}].$$

The experimental results are presented in Figures 8, 9 and 10. In Figure 8 is shown the time history of the contouring error e_C, which describes maximum peaks in steady state of 0.004 [m], a 2 % with respect to the circle radius. The path of the arm tip in the plane x_1–x_2 is depicted in Figure 9. The final circle traced by the arm tip presents slight deformations compared with the previous experiment (see Figure 6), but enhancement can be obtained by choosing higher gains. The time evolution of the tip speed $\|\dot{x}\|$ shown in Figure 10 has also high frequency components mainly due to velocity estimation and Coulomb friction. As in the test of the inverse dynamic based controller, smooth motion trasient was presented.

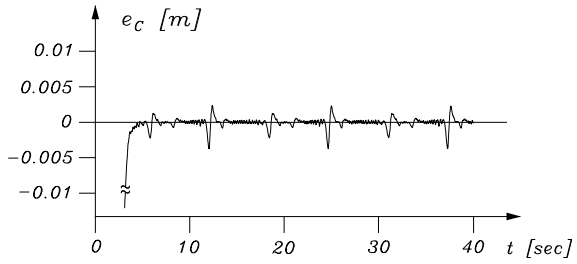

Fig. 8. Contouring error using two–loops based controller

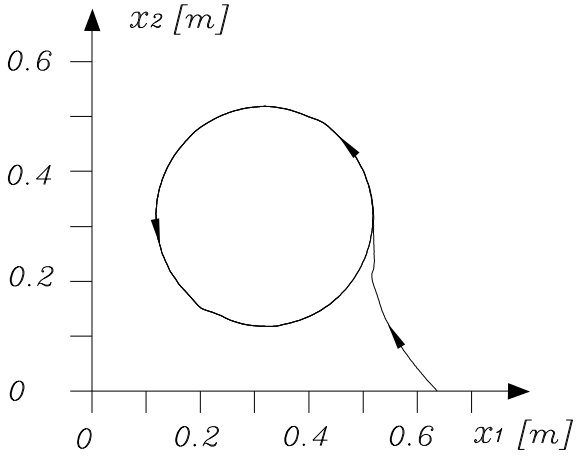

Fig. 9. Path of the arm tip using two–loops based controller

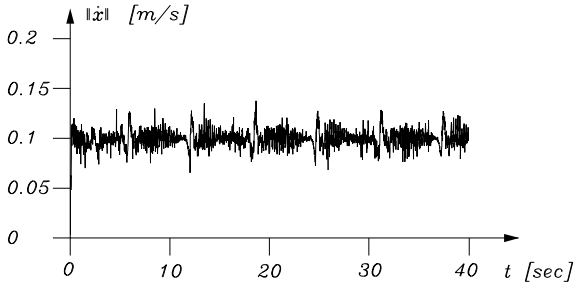

Fig. 10. Speed $\|\dot{x}\|$ using two–loops based controller

4. CONCLUSIONS

Velocity field control appears as an attractive alternative to control of manipulators when motion coordination among the robot axes is of concern. The desired motion of the manipulator is coded into a velocity field instead of the familiar description as trajectories depending on time. Two velocity field controllers have been proposed. In the experiments on a two degrees–of–freedom direct–drive arm presented, good performance in the contouring error and arm tip speed was observed without important difference between the two tested controllers. Coordinated motion was verified in the velocity field control approach.

5. REFERENCES

Canudas C., Siciliano B., Bastin G. (Eds.) (1996). *Theory of Robot Control*. Springer-Verlag, London, U.K.

Chiu, G. T.–C. (1998). Contour Tracking of Machine Tool Feed Drive Systems. In *Proc. of the American Control Conference*, Philadelphia, Pennsylvania, June, pp. 3833–3837.

Chiu, G. T.–C. and M. Tomizuka (2001). Contouring Control of Machine Tool Feed Drive Systems: A Task Coordinate Frame Approach. *IEEE Trans. on Control Systems Technology*, **9**, January, 130–131.

Kelly, R., Reyes, F., Moreno, J. and S. Hutchinson (1999). A Two Loops Direct Visual Control of Direct-Drive Planar Robots with Moving Target. In *Proc. of the International Conferences in Robotics and Automation*, Detroit, MI, May, pp. 599–604.

Li, P. and R. Horowitz (1999). Passive velocity field control of mechanical manipulators. *IEEE Trans. on Robotics and Automation*, **15**, 751–763.

Li, P. Y. (1999). Coordinated contour following control for machining operations – A survey. In *Proc. of the American Control Conference*, San Diego, CA., June, pp. 4543–4547.

Nakamura, M., Munasinghe, S. R., Goto, S. and N. Kyura (2000). Enhanced Contour Control of SCARA Under Torque Saturation Constraint. *IEEE/ASME Trans. on Mechatronics*, **5**, 437–440.

Reyes, F. and R. Kelly (1997). Experimental Evaluation of Identification Schemes on a Direct Drive Robot. *Robotica*, **15**, pp. 563–571.

Reyes, F. and R. Kelly (2001). Experimental evaluation of model–based controllers on a direct–drive robot arm. *Mechatronics*, **11**, 267–282.

Spong, M. W. and M. Vidyasagar (1989). *Robot Dynamics and Control*. John Wiley and Sons, New York, NY.